

Articles

Self-Assembled Electrooptic Superlattices. A Theoretical Study of Multilayer Formation and Response Using Donor–Acceptor, Hydrogen-Bond Building Blocks

Shahar Keinan, Mark A. Ratner,* and Tobin J. Marks*

Department of Chemistry and the Materials Research Center, Northwestern University,
2145 Sheridan Road, Evanston, Illinois 60208

Received November 12, 2003

The binding energies, electronic structures, and electrooptic responses of three donor– π -system–acceptor (triazine–vinylbenzylidene–barbituric acid) chromophores that display substantial molecular hyperpolarizabilities and are capable of forming hydrogen-bonded, self-assembled multilayers are investigated using DFT (geometry) and semiempirical (electronic structure) methods. The geometries of the monomers, head-to-tail dimers, and head-to-tail trimers are computed, as well as the linear optical properties and hyperpolarizabilities. Although all three monomers are found to be planar, self-assembly removes monomer planarity and the resulting complexes are slightly twisted. It is found that the combination of dipole moment alignment and short distances between the monomers results in the hyperpolarizabilities of the trimers being substantially greater than three times those of the corresponding monomers, evidencing a synergistic effect that enhances the electrooptic response.

Introduction

Electron donor–acceptor functionalized conjugated organic molecules can exhibit large electrooptic (EO) responses.^{1,2} Self-assembly of such molecules can be used to create highly ordered, microstructurally acentric, multilayer structures which are attractive for next-generation telecommunication, optical computing, and optical data storage technologies.^{2,3} A potentially attractive way of self-assembling large electrooptic response organic materials^{3,4} is by using directed intermolecular hydrogen-bonding interactions^{5,6} to organize

molecular connectivity.^{7–9} In principle, this can be achieved by appending hydrogen-bonding moieties to large-response NLO chromophore molecules. In a more sophisticated strategy, the donor and acceptor moieties of the conjugated chromophore molecule would simultaneously serve as hydrogen-bonding donors and acceptors, imparting microstructural stability and simplifying

* Authors to whom correspondence should be addressed. E-mail: t-marks@northwestern.edu, ratner@chem.northwestern.edu.

(1) For recent reviews of organic electrooptics, see: (a) *Molecular Nonlinear Optics: Materials, Phenomena and Devices*, Zyss, J., Ed. *Chem. Phys.* **1999**, 245 (Special issue). (b) *Measurement Techniques and Tabulations of Organic Nonlinear Optical Materials*, Kuzik, M. G., Dirk, C. W., Eds.; Marcel Dekker: New York, 1998. (c) Marder, S. R.; Kippelen, B.; Jen, A. K. Y.; Peyghambarian, N. *Nature* **1997**, 388, 845. (d) *Non-Linear Optical Materials: Theory and Modeling*, Karna, S. P., Yeates, A. T., Eds.; American Chemical Society: Washington, DC, 1996; Vol. 628. (e) *New Developments in Construction and Function of Organic Thin Films*, Möbius, D., Miller, R., Eds.; Elsevier: Amsterdam, 1996. (f) Zyss, J.; Nicoud, J. F. *Curr. Opin. Solid State Mater. Sci.* **1996**, 1 (4), 533. (g) *Molecular Nonlinear Optics-Materials, Physics and Devices*, Zyss, J., Ed.; Academic Press: San Diego, CA, 1994.

(2) (a) Luo, J.; Liu, S.; Haller, M.; Liu, L.; Ma, H.; Jen, A. K.-Y. *Adv. Mater.* **2002**, 14 (23), 1763. (b) Ma, H.; Jen, A. K.-Y. *Adv. Mater.* **2001**, 13 1201. (c) Bozec, H. L.; Douder, T. L.; Maury, O.; Bondon, A.; Ledoux, I.; Deveau, S.; Zyss, J. *Adv. Mater.* **2001**, 13, 1677. (d) Robinson, B. H.; Dalton, L. R. *J. Phys. Chem. A* **2000**, 104, 4785. (e) Shi, Y. Q.; Zhang, C.; Zhang, H.; Bechtel, J. H.; Dalton, L. R.; Robinson, B. H.; Steier, W. H. *Science* **2000**, 288, 119. (f) Huang, Q.; Kang, H.; Veinot, J.; Yan, H.; Zhu, P.; Marks, T. J. Nanoprecise Self-Assembly of Electro-Optic and Electroluminescent Molecular Arrays. In *Organic Nanophotonics*, Charra, F., Ed.; Kluwer Academic Publishers: Amsterdam, 2003.

(3) (a) Marks, T. J.; Ho, S. T.; Liu, Z.; Zhu, P.; Sun, D. Y.; Ma, J.; Xiao, Y.; Kong, H. *SPIE Proc.* **2003**, 4991, 133. (b) Zhao, Y.-G.; Chang, S.; Wu, A.; Lu, H.-L.; Ho, S. T.; van der Boom, M. E.; Marks, T. J. *Opt. Eng. Lett.* **2003**, 42, 298. (c) Facchetti, A.; Abbotto, A.; Beverina, L.; van der Boom, M. E.; Dutta, P.; Evmenenko, G.; Pagani, G. A.; Marks, T. J. *Chem. Mater.* **2003**, 15 (5), 1064. (d) Van Cott, K. E.; Guzy, M.; Neyman, P.; Brands, C.; Heflin, J. R.; Gibson, H. W.; Davis, R. M. *Angew. Chem., Int. Ed.* **2002**, 17, 3226. (e) van der Boom, M. E.; Zhu, P. W.; Evmenenko, G.; Malinsky, J. E.; Lin, W. B.; Dutta, P.; Marks, T. J. *Langmuir* **2002**, 18 (9), 3704. (f) Zhu, P. W.; van der Boom, M. E.; Kang, H.; Evmenenko, G.; Dutta, P.; Marks, T. J. *Chem. Mater.* **2002**, 14, 4982. (g) Facchetti, A.; Abbotto, A.; Beverina, L.; van der Boom, M. E.; Dutta, P.; Evmenenko, G.; Marks, T. J.; Pagani, G. A. *Chem. Mater.* **2002**, 14 (12), 4996. (h) Liu, Z.; Ho, S. T.; Chang, S.; Zhao, Y.; Marks, T. J.; Kang, H.; van der Boom, M. E.; Zhu, P. *Proc. SPIE* **2002**, 4798, 151. (i) Bakiamoh, S. B.; Blanchard, G. J. *Langmuir* **2001**, 17, 3438. (j) van der Boom, M. E.; Evmenenko, G.; Dutta, P.; Marks, T. J. *Adv. Funct. Mater.* **2001**, 11, 393. (k) Zhao, Y.-G.; Wu, A.; Lu, H.-L.; Chang, S.; Lu, W.-K.; Ho, S. T.; Van Der Boom, M. E.; Marks, T. J. *Appl. Phys. Lett.* **2001**, 79, 587. (l) Neff, G. A.; Helfrich, M. R.; Clifton, M. C.; Page, C. J. *Chem. Mater.* **2000**, 12, 2363. (m) Flory, W. C.; Mehrens, S. M.; Blanchard, G. J. *J. Am. Chem. Soc.* **2000**, 122, 7976. (n) Doron-Mor, H.; Hatzon, A.; Vaskevich, A.; van der Boom-Moav, T.; Shanzer, A.; Rubinstein I.; Cohen, H. A. *Nature* **2000**, 406, 382.

(4) Marks, T. J.; Ratner, M. A. *Angew. Chem., Int. Ed. Eng.* **1995**, 34, 155.

(5) (a) Sijbesma, R. P.; Meijer, E. W. *Chem. Commun.* **2003**, 5, (b) Zimmerman, S. C.; Corbin, P. S. Heteroaromatic Modules for Self-Assembly Using Multiple Hydrogen Bonds. In *Molecular Self-Assembly. Organic Versus Inorganic Approaches*, Fujita, M., Ed.; Springer: Berlin, 2000; Vol. 96, p 64.

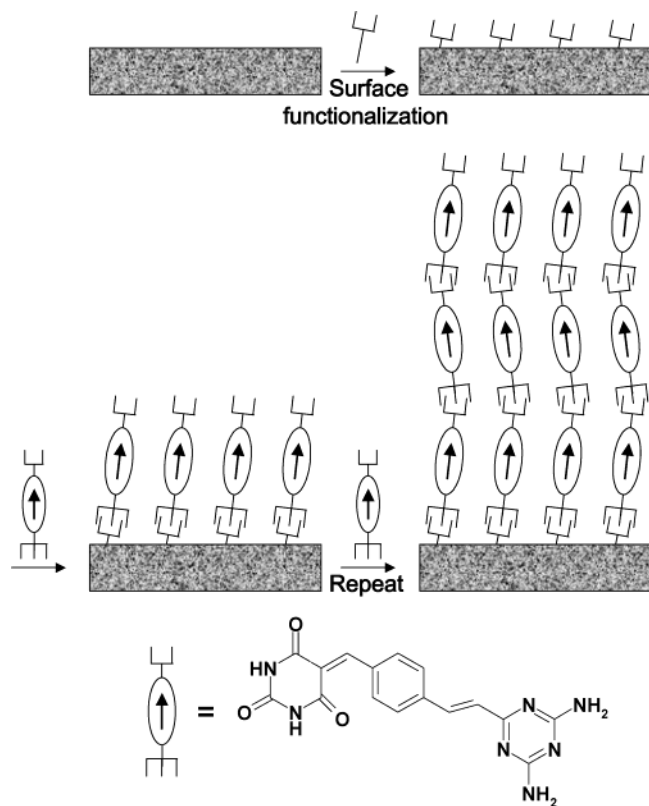
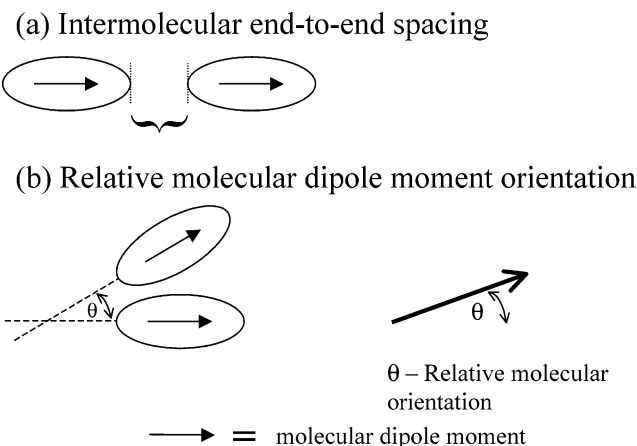


Figure 1. Self-assembly scheme for hydrogen-bonding chromophores on a functionalized surface.

the synthesis. In such an approach, the substrate surface for assembly would be functionalized with either a hydrogen-bond donor or acceptor template, followed by chromophore self-assembly on the functionalized surface, donor to acceptor, to form a multilayer (Figure 1). In principle, thin films could be grown either from the vapor phase¹⁰ or from solution. This approach to creating acentric optoelectronic multilayers represents a new strategy to ensure noncentrosymmetry, utilizing well-characterized connectivities, and furthermore offers the possibility of using intermolecular cooperative effects to enhance supramolecular electrooptic response.¹¹ However, any changes to the electronic structure of the chromophore molecules caused by the hydrogen-bonding interactions are also likely to influence the EO response and should be anticipated in advance.

It is the focus of this contribution to investigate the stabilities and EO responses of potential multilayer self-assembling hydrogen-bonded materials and to ascertain

Chart 1. Factors Influencing Bulk Hyperpolarizability: (a) Intermolecular Distance and (b) Relative Molecular Orientation



whether chromophore connectivities can be used to enhance the EO response of chromophore aggregates. Here the growing capabilities of first-principles methods offer many advantages in the rational design of new materials. This contribution theoretically investigates “real case” molecules which can be NLO-active and can also self-assemble via direct hydrogen bonding, and suggests ways to tune the hyperpolarizability properties. The experimental aspects of this strategy are discussed separately.¹²

There have been several theoretical investigations of the changes in molecular hyperpolarizability (β) induced by weak intermolecular interactions such as hydrogen bonding. Some of these examples deal with “model” molecules such as the water dimer¹³ or a linear array of HF molecules,¹⁴ whereas other studies have focused on the urea crystal structure^{15,16} or *para*-nitroaniline dimers.^{14,17} From these investigations, it is evident that several factors influence the changes in hyperpolarizability on proceeding from monomer to dimer or cluster; the two most influential factors are the end-to-end intermolecular separation and the relative molecular dipole orientation (Chart 1). To achieve a net effective enhancement in aggregate β value, the component molecular dipole moments should be aligned in a head-to-tail position, and for this orientation, β increases with decreasing end-to-end and/or intermolecular distance.^{17,18} Using hydrogen-bonding to self-assemble large-response NLO chromophores as in Figure 1 coincides well with these strategies for increasing β . First, the directionality of hydrogen bonding predetermines that the molecules be oriented in a specific manner^{5,6} (preferably with the molecular dipole moments aligned). Second, hydrogen bonding promotes closer molecular approach,¹⁹ more than that in other weakly bound systems, thereby achieving significant net enhancement in response.

(6) (a) Prins, L. J.; Reinhoudt, D. N.; Timmerman, P. *Angew. Chem., Int. Ed.* **2001**, *40*, 2382. (b) Beijer, F. H.; Sijbesma, R. P.; Kooijman, H.; Spek, A. L.; Meijer, E. W. *J. Am. Chem. Soc.* **1998**, *120*, 6761. (c) Beijer, F. H.; Sijbesma, R. P.; Vekemans, J. A. J. M.; Meijer, E. W.; Kooijman, H.; Spek, A. L. *J. Org. Chem.* **1996**, *61*, 6371. (d) Lawrence, D. S.; Jiang, T.; Levett, M. *Chem. Rev.* **1995**, *95*, 2229. (e) Whitesides, G. M.; Simanek, E. E.; Mathias, J. P.; Seto, C. T.; Chin, D. N.; Mammen, M.; Gordon, D. M. *Acc. Chem. Res.* **1995**, *28*, 37.

(7) Johal, M. S.; Cao, Y. W.; Chai, X. D.; Smilowitz, L. B.; Robinson, J. M.; Li, T. J.; McBranch, D.; Li, D. *Chem. Mater.* **1999**, *11*, 1962.

(8) Saadeh, H.; Wang, L.; Yu, L. *J. Am. Chem. Soc.* **2000**, *122*, 546.

(9) Pal, S. K.; Krishnan, A.; Das, P. K.; Samuelson, A. G. *J. Organomet. Chem.* **2001**, *637–639*, 827.

(10) (a) Cai, C.; Bösch, M. M.; Müller, B.; Tao, Y.; Kündig, A.; Bosshard, C.; Gan, Z.; Biaggio, I.; Liakatas, I.; Jäger, M.; Schwer, H.; Günter, P. *Adv. Mater.* **1999**, *11*, 745. (b) Cai, C.; Bösch, M. M.; Tao, Y.; Müller, B.; Gan, Z.; Kündig, A.; Bosshard, C.; Liakatas, I.; Jäger, M.; Günter, P. *J. Am. Chem. Soc.* **1998**, *120*, 8563.

(11) Kakkar, A. K.; Yitzchaik, S.; Roscoe, S. B.; Kubota, F.; Allan, D. S.; Marks, T. J. *Langmuir* **1993**, *9*, 388.

(12) (a) Zhu, P.; Kang, H.; Facchetti, A.; Evmenenko, G.; Dutta, P.; Marks, T. J. *Polym. Prepr.*, accepted for publication. (b) Zhu, P.; Facchetti, A.; Kang, H.; Evmenenko, G.; Dutta, P.; Marks, T. J. *J. Am. Chem. Soc.* **2003**, *125*, 11496.

(13) Maroulis, G. *J. Chem. Phys.* **2000**, *113*, 1813.

(14) Moliner, V.; Escibano, P.; Peris, E. *New J. Chem.* **1998**, 387.

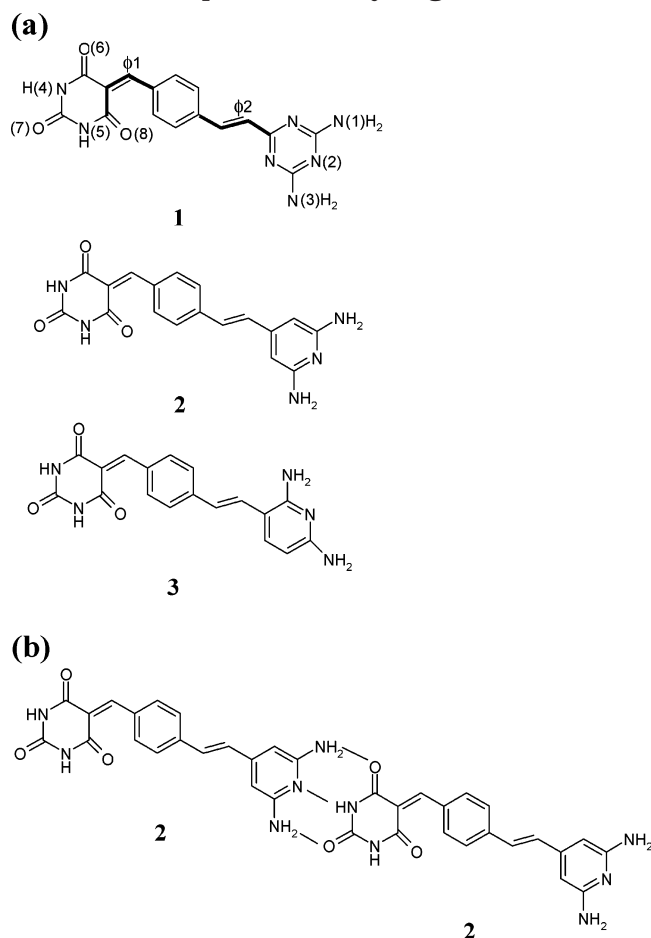
(15) Reis, H.; Papadopoulos, M. G.; Munn, R. W. *J. Chem. Phys.* **1998**, *109*, 6828.

(16) Wu, K.; Snijders, J. G.; Lin, C. *J. Phys. Chem. B* **2002**, *106*, 8954.

(17) Di Bella, S.; Ratner, M. A.; Marks, T. J. *J. Am. Chem. Soc.* **1992**, *114*, 5842.

(18) Jensen, L.; Astrand, P. O.; Osted, A.; Kongsted, J.; Mikkelsen, K. V. *J. Chem. Phys.* **2002**, *116*, 4001.

Chart 2. (a) Chromophores Combining Hydrogen-Bonding Capacities with Large Electrooptic Response. Labels Show Important Dihedral Twist Angles (see more specific numbering scheme in Table 2b) and Hydrogen-Bonding Atoms. (b) Dimerization of Chromophore 2 via Hydrogen Bonds



The electrooptic response of bulk molecular materials is governed by the properties of the individual molecules, by their interaction with the neighboring molecules, and by overall microstructural organization. Therefore, to understand the response properties of the bulk materials, an analysis of molecular response vis-à-vis the response of molecular aggregates should first be made, so that an efficient atomistic level design procedure for optical molecular materials can be achieved. Chromophore molecules **1**–**3** shown in Chart 2 were chosen for study in this work. In chromophore **2**, the triazine moiety of chromophore **1** is changed to a 2,4-diamino-pyridine moiety, while in chromophore **3** it is changed to a 1,3-diamino-pyridine moiety. All three monomers have the same triple hydrogen-bonding capacities, however their NLO response properties differ significantly, so that comparison should be informative. These molecules are part of an ongoing experimental/modeling rational materials design effort program in

Table 1. Energies of Chromophores and H-Bonded Chromophore Dimers and Trimers

structure	E(DFT) ^a [H]	E(Def) ^b [kcal/mol]	E(Int) ^c [kcal/mol]	E(Sta) ^d [kcal/mol]
1	−1226.6287			
1·1	−2453.2813	1.63	−14.95	−13.32
1·1·1	−3679.9336	3.45	−29.70	−26.25
2	−1194.5166			
2·2	−2389.0505	4.20	−10.84	−6.63
2·2·2	−3583.5900	6.46	−25.24	−18.78
3	−1194.5180			
3·3	−2389.0596	0.09	−14.81	−14.71
3·3·3	−3583.6011	1.88	−29.52	−27.64

^a E(DFT) is the total energy in Hartrees of the complexes (geometry optimization using DFT/B3LYP/6-31G**, energy calculated using DFT/B3LYP/6-31G**++). ^b E(Def) is the energy difference between the monomer minimal energy conformation and the corresponding monomers in the complex. ^c E(Int) is the energy difference between the complex and the corresponding monomeric precursors, each in the minimal energy geometry. ^d E(Sta) is the sum of the interaction and deformation energy for each complex. Also shown is E(Int) in kcal/mol, for comparison purposes.

this laboratory.¹² They are prepared from known building blocks that are widely used for self-assembled hydrogen-bonding systems.^{5,6} Both the properties of the triple hydrogen-bonding connectors^{5,20} and the molecular EO properties^{1,2,21} of the chromophoric cores have been separately demonstrated in the past.

Computational Details

Models of the isolated gas-phase molecules were constructed with the Maestro program. Initial geometry optimization was carried out with the UFF option in the Jaguar²² program. The resulting structures were then subjected to unrestricted geometry optimization using the B3LYP^{23,24} DFT hybrid method with the 6-31G** basis set as implemented in the Jaguar program.²² The monomer equilibrium geometries were used to construct the starting geometries of the corresponding dimer and trimer for each molecule. The dimers and trimers were then optimized using the same procedure as for the monomer. To evaluate better the hydrogen-bonding affinities and to overcome basis set superposition error (BSSE), the single point energies of the equilibrium geometries were also calculated with the 6-31G**++ basis set. Table 1 summarizes results of the calculations. In this work, hydrogen bonding is discussed only in terms of observable properties such as geometry, metrical parameters, interaction energies, and optical properties; the nature of the hydrogen bonds per se will not be addressed here.

The first hyperpolarizability β appears as a third rank tensor in the first nonlinear term that arises in the dependence of the molecular induced dipole moment μ on the applied electric field F experienced by the molecule:²⁵

$$\mu_i = \mu_i^{(0)} + \sum_j \alpha_{ij} F_j + \left(\frac{1}{2} \right) \sum_{j,k} \beta_{ijk} F_j F_k \quad (1)$$

Here $\mu_i^{(0)}$ is the permanent dipole moment of the

(19) Jeffrey, G. A. *An Introduction to Hydrogen Bonding*; Oxford University Press: New York, 1997.

(20) Krische, M. J.; Lehn, J.-M. The Utilization of Persistent H-Bonding Motifs in the Self-Assembly of Supramolecular Architectures., In *Structure & Bonding: Molecular Self-Assembly. Organic versus Inorganic Approach*; Fujita, M., Ed.; Springer-Verlag: Berlin, 2000; Vol. 96, p 3.

(21) Beratan, D. N. Electronic Hyperpolarizability and Chemical Structure. In *Materials for Nonlinear Optics: Chemical Perspective*; Marder, S. R., Sohn, J. E., Stucky, G. D., Eds.; American Chemical Society: Washington, DC, 1991; Vol. 455, p 89.

(22) Jaguar. Jaguar 4.2; Schrödinger, Inc.: Portland, OR, 1991–2000.

(23) Becke, A. D. *Phys. Rev. A* **1988**, *38*, 3098.

(24) Lee, C.; Yang, W.; Parr, R. G. *Phys. Rev. B* **1988**, *37*, 785.

molecule in direction i , F_j is the component of the electromagnetic field in the j direction, and α and β are the static (zero frequency, $\omega = 0.0$ eV) first- and second-order polarizability tensors, as a function of the field strength. We will concentrate on the process of frequency doubling, also called second harmonic generation. To avoid issues of resonance enhancement, we report only the limiting zero frequency or "static" case ($\omega = 0.0$ eV):

$$\beta_{SHG} = \beta(-2\omega; \omega, \omega) \quad (2)$$

We are interested in the β_{tot} component of the β tensor:

$$\beta_{tot} = \sqrt{\beta_x^2 + \beta_y^2 + \beta_z^2};$$

$$(\beta_i = \beta_{iii} + (1/3) \sum_{j \neq i} (\beta_{ijj} + \beta_{jji} + \beta_{jjj})) \quad (3)$$

The calculated equilibrium geometries were used to compute spectral properties within the *CNDO*²⁶ program, using the spectroscopic INDO/S²⁷ semiempirical model with the CI active space of all single excitations between the 55 orbitals below the HOMO and 55 orbitals above the LUMO. Nonlinear optical responses (β) were evaluated by the SOS²⁸ method, using the *CNDO* program output. The SOS program was written in-house. Molecular dipole moments were also calculated at this level of theory. This computational scheme has demonstrated the ability to predict, accurately, the linear optical and NLO response properties of diverse organic chromophore classes.²⁹ The large CI window was chosen to include all active orbitals for the increasing size of the monomers, dimers, and trimers, after systematically increasing the CI windows size and ascertaining whether the optical and hyperpolarizability properties have converged.

Results and Discussion

We present here the results of the calculations carried out on the three triazine–vinylbenzylidene–barbituric acid donor– π -system–acceptor chromophores (Chart 2).¹² Part I will investigate geometrical changes accompanying complexation of these chromophores by comparing monomer, dimer, and trimer molecular structures. In Part II, energetic changes upon complexation will be examined. Part III will describe linear optical response, and Part VI will cover the hyperpolarizabilities of the monomers and complexes of the three chromophores.

I. Molecular and Hydrogen-Bonded Cluster Geometries. The first stage in understanding the interplay between hydrogen-bonding and chromophore electronic structure is scrutinizing the molecular cluster geometry. Using semiempirical methods such as PM3 or AM1 is not always sufficiently accurate, and one must use first-principles methods such as DFT or HF/MP2

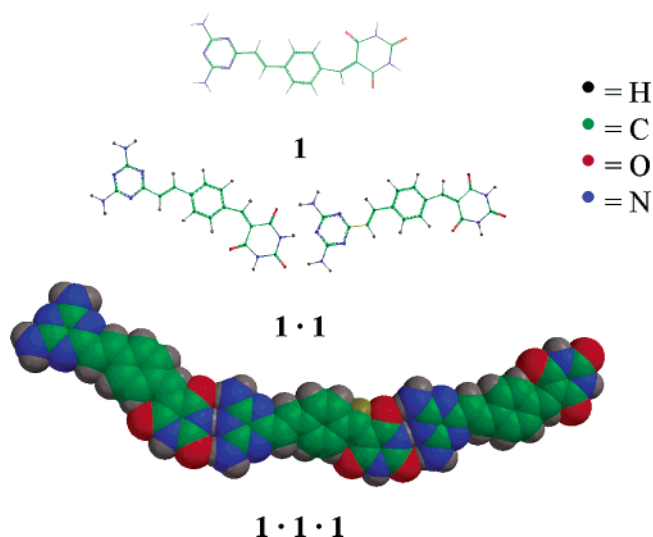


Figure 2. DFT/B3LYP/6-31G** minimal energy geometry of chromophore **1** monomer (top), dimer (center), and trimer (bottom).

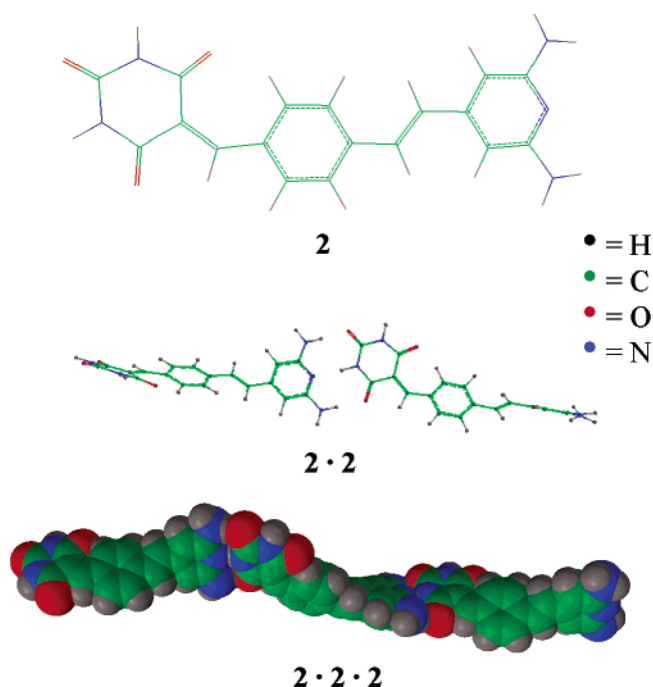


Figure 3. DFT/B3LYP/6-31G** minimal energy geometry of chromophore **2** monomer (top), dimer (center), and trimer (bottom).

to obtain accurate cluster geometries.^{30,31} Figures 2, 3, and 4 show the DFT/B3LYP/6-31G** geometry-optimized structures of the monomer, as well as the hydrogen-bonding-connected head-to-tail dimer and trimer of each chromophore molecule. Table 2a compiles selected hydrogen-bond lengths and X–H...Y angles for the complexes, and Table 2b compiles selected dihedral twist angles for the complexes. Here ϕ_1 , as defined in Chart 2, is the dihedral angle involving carbon atoms 9,10,11,12, and ϕ_2 is the dihedral angle involving carbon atoms 13,14,15,16. While all three free monomers are found to be rigorously planar, complex formation removes the planarity (Table 2b) via twisting about bonds

(25) Boyd, R. W. *Nonlinear Optics*; Academic Press: San Diego, 1992.

(26) Zeng, J.; Hush, N. S.; Reimers, J. R. *J. Am. Chem. Soc.* **1996**, *118*, 2059.

(27) Ridley, J.; Zerner, M. *Theor. Chim. Acta* **1973**, *32*, 111.

(28) Orr, B. J.; Ward, J. F. *Mol. Phys.* **1971**, *20*, 513.

(29) Albert, I. S. D.; Marks, T. J.; Ratner, M. A. Practical Computational Approaches to Molecular Properties. In *Characterization Techniques and Tabulations for Organic Nonlinear Optical Materials*; Kuzyk, M. G., Dirk, C. W., Eds.; Marcel Dekker: New York, 1998; p 37.

(30) Guerra, C. F.; Bickelhaupt, F. M.; Snijders, J. G.; Baerends, E. J. *J. Am. Chem. Soc.* **2000**, *122*, 4117.

(31) Lukin, O.; Leszczynski, J. *J. Phys. Chem. A* **2002**, *106*, 6775.

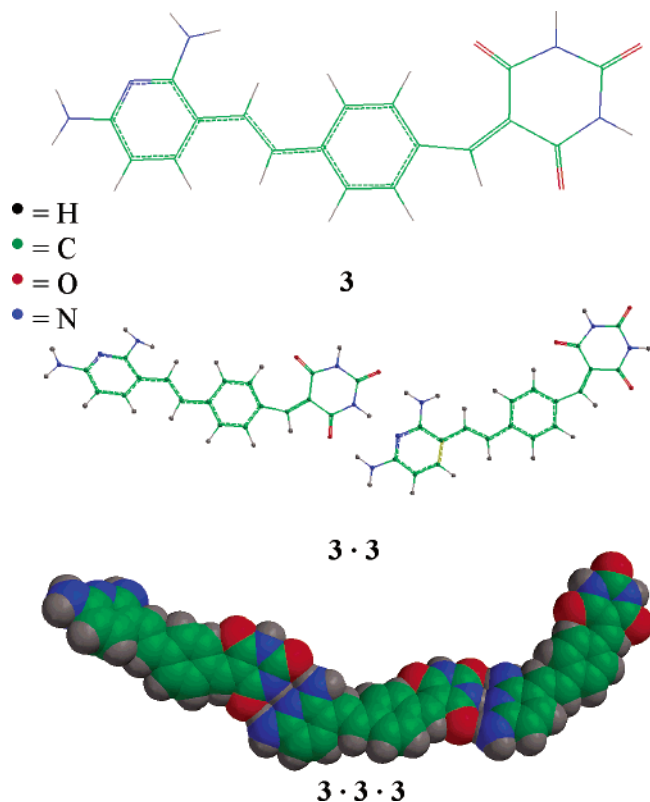


Figure 4. DFT/B3LYP/6-31G** minimal energy geometry of chromophore **3** monomer (top), dimer (center), and trimer (bottom).

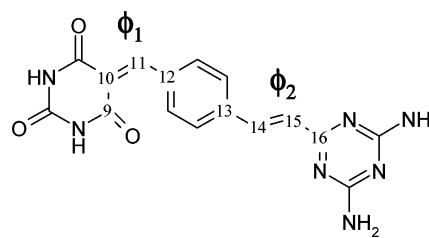
ϕ_1 , C10–C11, and ϕ_2 , C14–C15 (probably due to electron deficiency in the aromatic rings, which lowers conjugation in the triazine–vinylbenzylidene π -system and thus allows distortion). For chromophore **1**, the deviation from planarity is negligible; however, for chromophore **3**, and more markedly for chromophore **2**, large deviations from planarity upon complex formation are computed. The nonplanarity of the dimer of chromophore **2** arises not from the triple hydrogen-bonds, which are nearly planar, but, as noted above, from the molecular dihedral angles about two double bonds (the one connecting the pyridine and phenylene ring, ϕ_2 , and the one connecting the phenylene ring to the barbituric acid ring, ϕ_1) which are approximately 10° each. Such a change from planar monomer to nonplanar complex is also found in DNA base pairs.³²

Another metrical observation in this work is that bonds to atoms participating in hydrogen bonding are elongated (Table 2), due to sharing of the hydrogen atom between the hydrogen donor and acceptor, as one would expect.¹⁹ For example, the N(4)–H bond length (see Chart 2 for atom labeling scheme) increases from 1.01 Å in the free monomer to 1.05 Å in the trimer of chromophore **3**, and the C–O(7) bond length increases from 1.21 Å in the free monomer to 1.23 Å in the trimer of chromophore **3**. The N(5)–H bond length in the trimer of chromophore **3** remains 1.01 Å upon complexation because N(5) does not participate in hydrogen bonding. The same behavior is found for other dimers and trimers in this series. These kinds of changes are similar to those observed, both experimentally and in theoretical studies, for neutral organic hydrogen bonds.¹⁹

Table 2. Selected Calculated Intermolecular Distances and Angles in the DFT/B3LYP/6-31G** Optimized Geometries of Chromophore Dimers and Trimers^a

Table 2a			
structure	H-bond pairs	H-bond length [Å]	X–H···Y bond angle [°]
1·1	N(1)–O(6)	2.94	175
	N(2)–N(4)	2.88	179
	N(3)–O(7)	2.95	175
2·2	N(1)–O(6)	2.95	171
	N(2)–N(4)	2.92	171
	N(3)–O(7)	2.96	170
3·3	N(1)–O(6)	2.92	179
	N(2)–N(4)	2.98	179
	N(3)–O(7)	2.91	174
1·1·1	N(1)R–O(6)M	2.96	175
	N(2)R–N(4)M	2.87	178
	N(3)R–O(7)M	2.91	175
	N(1)M–O(6)L	2.94	175
	N(2)M–N(4)L	2.90	179
	N(3)M–O(7)L	2.94	176
2·2·2	N(1)R–O(6)M	2.97	177
	N(2)R–N(4)M	2.91	174
	N(3)R–O(7)M	2.92	170
	N(1)M–O(6)L	2.96	167
	N(2)M–N(4)L	2.90	171
	N(3)M–O(7)L	2.95	172
3·3·3	N(1)R–O(6)M	2.89	176
	N(2)R–N(4)M	2.96	176
	N(3)R–O(7)M	2.91	173
	N(1)M–O(6)L	2.90	177
	N(2)M–N(4)L	2.98	178
	N(3)M–O(7)L	2.94	176

Table 2b



structure	monomer	ϕ_1 [°]	ϕ_2 [°]
1·1	L	0	0
	R	0	0
2·2	L	1	9
	R	3	2
3·3	L	1	3
	R	2	7
1·1·1	L	1	0
	M	2	1
2·2·2	R	1	0
	L	2	1
3·3·3	M	1	9
	R	8	1
	L	2	5
	M	0	4
	R	5	7

^a For the trimers, the atom labeling includes the monomer location: R (right monomer), M (central monomer), and L (left monomer)

For chromophore **3**, in both the dimeric and trimeric complexes, the N–H···N hydrogen bonds are longer than the O–H···N hydrogen bonds; whereas for chromophores **1** and **2** the opposite trend is seen. N–H···N hydrogen bonds are usually longer than O–H···N hydrogen bonds because the O atom has smaller covalent and van der Waals radii and greater electronegativity than the N atom. However, other factors, such as steric hindrance and electrostatic interactions, also play an important role.³²

II. Hydrogen-Bonded Complex Stabilization Energetics. The following energy contributions were

(32) Sponer, J.; Leszczynski, J.; Hobza, P. *J. Phys. Chem.* **1996**, *100*, 1965.

Table 3. Optical Excitation Energies in eV of the Indicated Monomers, Dimers, and Trimers of Each Chromophore

chromophore	monomer	dimer	trimer
1	3.47	3.54	3.52
2	3.37	3.45	3.51
3	2.91	2.90	2.83

computed: E(DFT), the total energy in Hartrees of the complexes; E(Def), the deformation energy of a monomer upon complexation, defined as the difference in the energy of the monomer minimal energy conformation and the energy of the monomer having the same geometry as within the complex. E(Int) is the interaction energy, the energy difference between the complex and the corresponding monomeric precursors, all computed in minimum energy geometries. E(Sta), the stabilization energy, was calculated as the sum of the interaction energies and the deformation energies of the complex. A summary of the results can be found in Table 1.

The strength of hydrogen bonding between the monomers can be evaluated using the interaction energy, E(Int). All dimers have three component hydrogen bonds and trimers have six component hydrogen bonds, so that the average single hydrogen-bond strength is ~ 5 kcal/mol for complexes of **1** and **3**, and ~ 4 kcal/mol for complexes of **2** (experimental measurements of hydrogen-bond strengths yield 4–15 kcal/mol¹⁸). The differences in bond energies can be attributed to the hydrogen-bonding geometry: although the average hydrogen-bond lengths (2.92–2.94 Å) are similar, the average bond angle suggests weaker hydrogen bonds in chromophore **2** (170° vs 176° for **1** and **3** complexes). This is, again, not completely unexpected.¹⁸

All of the present chromophore complexes have the same number and types of hydrogen bonding and secondary interactions, so that the differences in the total complex stability are due to the hydrogen-bonding geometry and monomer structural deformations. The complexes of **2** are more distorted than the complexes of **1** and **3**, as indicated in the larger deformation energies of the chromophore **2** complexes (Table 1). Both the interaction and deformation energies contribute to the differences in complex stabilization energy, where the complexes of chromophores **1** and **3** are more stable than those of chromophore **2**.

III. Linear Optical Response Properties. The optical properties of a hydrogen-bonded chromophore complex should resemble those of the component monomers, with slight perturbations. For example, homodimers usually display red-shifted excitation energies in comparison to those of the monomer, due to interaction between the two chromophore dipole moments that stabilize molecular orbital energies, usually stabilizing the excited state more than the ground state, thus decreasing the orbital gaps.¹⁷ Table 3 shows the excitation energies of the present monomers, dimers, and trimers. The excitation energies for chromophore **3** are red-shifted upon complexation, as expected. Interestingly, however, the excitation energies of chromophores **1** and **2** are blue-shifted. For hydrogen-bonded molecules, the appearance of both red-shifted and blue-shifted optical excitations has been observed before.³³ Although there is still debate in the literature as to the origin of these phenomena,^{34,35} it is of interest to

Table 4. Calculated Total Dipole Moments (in Debye) of the Indicated Monomer, Dimers, and Trimers for Each Chromophore, Calculated at the DFT/B3LYP/6-31G Level**

chromophore	monomer	dimer	trimer
1	6.0	11.7	15.2
2	4.3	6.0	9.8
3	7.3	15.4	22.6

Table 5. Computed β_{tot} ($\omega = 0.0$ eV) in 10^{-30} cm⁵/esu of the Indicated Monomers, Dimers, and Trimers of Each Chromophore

chromophore	monomer	dimer	trimer
1	15.8	12.9	30.8
2	24.7	40.4	60.9
3	60.3	121.3	210.8

compare the molecular dipole moments to those of the complexes and to determine whether there is any correlation with the shifts in the optical spectra. Table 4 shows the calculated total dipole moments (in Debyes) of the monomer, dimers, and trimers for each of the present chromophores. Both chromophore **1** and **2** exhibit a decrease in dipole moment upon complexation, which is accompanied by a blue-shift of the first optical excitation, whereas chromophore **3** displays an increase of the total dipole moment upon complexation, accompanied by a red-shifted excitation. These results are in accord with expectations based on classical coupling of dipoles, however more detailed examination of the differences between the ground and excited-state dipole moments is needed before more quantitative arguments can be made.

IV. Monomer and Complex Hyperpolarizabilities. As noted in the Introduction, the effects of delocalization, increased dipole moment, and shifts in optical excitation energies suggest that the NLO response may increase upon hydrogen-bond complexation. In Table 5, the computed hyperpolarizabilities of the monomer, head-to-tail dimer, and head-to-tail trimer of each chromophore are given. It is evident from these results that for chromophore **3** the above qualitative expectation is essentially correct—a far greater nonlinear response is observed for the trimer **3·3·3** vs the corresponding sum of the monomer responses, and there is a distinct enhancement in NLO response over the simple sum of the individual molecular contributions, with a gain of $\Delta\beta = 30 \times 10^{-30}$ cm⁵/esu (trimer – 3*monomer). Here, as in the optical spectra of the complexes, the importance of the correct alignment of the monomer dipole moments becomes clear. When the chromophore dipole moments are aligned to enhance the net dipole moment, there is a synergistic effect that enhances the hyperpolarizability of the complex compared to that of the individual monomer units. However, if the chromophores are aligned to reduce the net dipole moment, as observed for the dimer and trimer of chromophores **1** and **2**, then there is no synergistic effect, and the total hyperpolarizability is reduced.

Is the decrease in β a result of dipole moment alignment, or of molecular backbone twisting, thus lowering molecular conjugation and individual monomer hyperpolarizability? This question can be rephrased to whether the source of the decrement in β is a molecular

(33) Besley, N. A.; Hirst, J. D. *J. Am. Chem. Soc.* **1999**, *121*, 8559.(34) Scheiner, S.; Kar, T. *J. Phys. Chem. A* **2002**, *106*, 1784.(35) Qian, W.; Krimm, S. *J. Phys. Chem. A* **2002**, *106*, 6628.

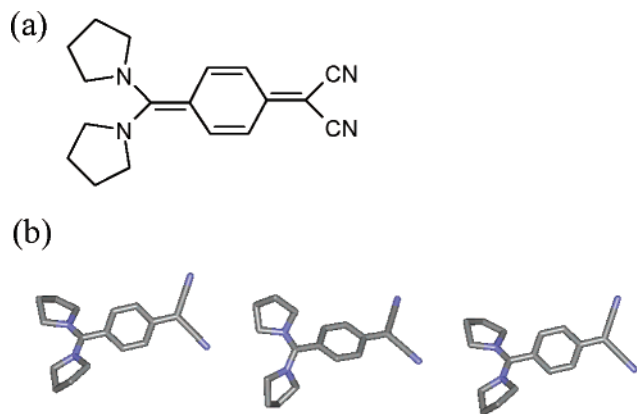
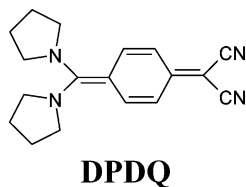


Figure 5. (a) Molecular structure of 7,7-dipyrrolidino-8,8-dicyanoquinodimethane (DPDQ). (b) DPDQ packing as found in the crystal structure. The hydrogen atoms are omitted for clarity.

or supramolecular phenomenon. To resolve this issue, an artificial dimer of chromophore **2** was constructed from two planar monomers (each identical to geometry-optimized chromophore **2**), but with the same hydrogen-bond metrics (distances) as in the geometry-optimized one. The nonlinear optical properties of this dimer, **planar-2-2**, were then calculated and compared to those of the geometry-optimized structure. It is found that $\beta_{\text{tot}}(\text{planar-2-2}) = 44.6 \times 10^{-30} \text{ esu}$, which is larger than $\beta_{\text{tot}}(\text{2-2}) = 40.46 \times 10^{-30} \text{ esu}$ of the geometry optimized dimer, but still not equal to that of two monomers, $2\beta_{\text{tot}}(\text{2}) = 49.4 \times 10^{-30} \text{ esu}$. Thus, one can conclude that twisting the monomers upon dimerization will lower molecular conjugation, and thus lower the dimer β_{tot} .



How important are the hydrogen-bonding metrics to the observed enhancement of β ? Besides aligning the molecular dipole moments, hydrogen-bonded molecules can achieve much closer proximities than van der Waals distances. To investigate this issue further, we compare our calculations on complexes of **1-3** to the computed response of a fragment of an archetypical NLO-active crystal structure. The smallest intermolecular contact in the present hydrogen-bonded complexes is $\sim 1.8\text{--}2.0 \text{ \AA}$ ($\text{N}(2)\cdots\text{H}-\text{O}(6)$), which is much shorter than in a typical NLO-active molecular crystal where intermolecular contacts are usually $\geq 3.0 \text{ \AA}$. An example is acentric 7,7-dipyrrolidino-8,8-dicyanoquinodimethane, DPDQ³⁶ (Figure 5). We used the published, diffraction-derived coordinates to select lattice fragments containing 1 to 3 DPDQ units. The particular fragments were chosen to minimize the intermolecular contacts, while keeping the monomer dipole moments aligned (see Figure 5). The smallest distance between individual monomers is 2.8 \AA ($\text{C}-\text{N}\cdots\text{H}$ -pyridine), and the molecular dipole moments are aligned in a "head-to-tail" fashion (Figure 5b). β_{tot} was calculated for each DPDQ

aggregate and it is found that there is a *net reduction* in hyperpolarizability per unit on going from monomer to dimer to trimer: $\beta_{\text{tot}}(\text{monomer}) = 102.6 \times 10^{-30} \text{ esu}$; $\beta_{\text{tot}}(\text{dimer}) = 174.5 \times 10^{-30} \text{ esu}$; $\beta_{\text{tot}}(\text{trimer}) = 253.1 \times 10^{-30} \text{ esu}$. The dipole moments, however, are the sum of the dipole moments of monomers: $\mu(\text{monomer}) = 24.8 \text{ D}$; $\mu(\text{dimer}) = 52.2 \text{ D}$; $\mu(\text{trimer}) = 79.1 \text{ D}$. In this case, although the dipole moments are aligned, the distance between monomers is too long, there are no synergistic effects between them, and the net hyperpolarizability decreases. Intermolecular distances in hydrogen-bonded systems are shorter, and the monomers interact so that synergistic effects increase the hyperpolarizability of the entire complex. It can be concluded that both alignment of the monomer dipole moment and close proximity between the aligned monomers will enhance β .

Conclusions

We have computed the molecular structures and electronic properties of monomers, head-to-tail dimers, and head-to-tail trimers of three triazine-vinylbenzylidene-barbituric acid donor-acceptor π -system chromophores that can undergo self-assembly via triple hydrogen bonding. All of the hydrogen-bonded complexes are more stable than the monomers, with average single hydrogen-bond strengths of $\sim 4\text{--}5 \text{ kcal/mol}$. The stability of the hydrogen-bonded systems is a result of many contributions, such as hydrogen-bond length and linearity, and molecular distortion, which are coupled, compensate mutually, and cannot be fully separated or isolated. For the systems studied here, the monomers undergo some distortion from planarity upon complexation, and the deformation energy cost lowers the stabilization energy of the complexes, especially for chromophore **2**. Strong interaction energies result from the linear, short hydrogen bonds found in the case of chromophores **1** and **3**.

The three chromophores investigated display differing molecular second-order electrooptic responses, from relatively weak (chromophore **1**) to strong (chromophore **3**). The complexes of chromophore **3** show substantial enhancements of β upon oligomerization via head-to-tail hydrogen-bond formation in comparison to that of the monomers, resulting from dipole moment alignment and short distances between monomers. To realize an efficient organic electrooptic modulator^{1,2} starting from a large-response NLO monomer, it is essential to maximize the bulk electrooptic response. Hydrogen-bond formation enhances the hyperpolarizability because it increases intermolecular bonding and decreases the distance between monomer dipole moments. We have now shown that connecting molecules using intermolecular hydrogen bonding is a potentially useful way of enhancing β .

Acknowledgment. This work was partially supported by the National Computational Science Alliance under grant number CHE020035N (small allocation account). This work was supported by the MURI program of the DoD, by the Materials Division of the NSF through the Northwestern MRSEC (grant DMR-0076077), and by DARPA/ARO (DAAD 19-00-1-0368). S.K. thanks Drs. A. Israel and P. Zhu for helpful discussions. We are grateful to J. Reimers for his CNDO program.

(36) Ravi, M.; Rao, D. N.; Cohen, S.; Agranat, I.; Radhakrishnan, T. P. *Chem. Mater.* **1997**, *9*, 830.